LRP 679/00 October 2000

Stability and α-Particle Confinement in the Sphellamak Reactor Concept

W.A. Cooper and O. Fischer

ISSN 0458-5895

STABILITY AND α-PARTICLE CONFINEMENT IN THE SPHELLAMAK REACTOR CONCEPT

W. Anthony Cooper and Olivier Fischer,
EPFL – Centre de Recherches en Physique des Plasmas

Abstract

Le Sphellamak est un système hybride sans noyau central composé par des éléments de Tokamak, de Stéllérateur et de Sphéromak. L'absence de colonne centrale permet la réalisation d'un système toroïdal compact puisque le manteau de protection interne ne devient plus nécessaire. Avec un profil de courant piqué, une séquence d'équilibres Sphellamak de dimension réacteur est calculée numériquement en variant le courant des bobines helicoïdales I_{hc} tout en fixant le courant toroïdal du plasma $I_p = -30MA$ ainsi que la moyenne volumique $\beta = 7.3\%$. Les modes globaux externes du type *kink* sont faiblement instables mais suffisent à garantir la stabilité pour $I_{hc} > 138MA$. Les critères de stabilité magnétohydrodynamique idéale locale sont réalisés pour des courants de $42MA < I_{hc} < 122MA$. Le courant toroïdal piqué produit localement des valeurs maximales pour le module du champs magnétique dans la région centrale du plasma ce qui implique des conditions favorables pour le confinement des particules énergétiques et thermiques. Cette conclusion est confirmée à travers le calcul d'un taux de perte très faible des orbites du centre de guidage des particules α.

The Sphellamak is a coreless hybrid system with Tokamak, Stellarator and Spheromak features. The absence of a central conductor permits the realisation of a compact toroidal system as internal shielding becomes unnecessary. With a peaked toroidal current profile, a sequence of reactor-sized Sphellamak equilibria is computed numerically in which the current in the helical coils I_{hc} is varied while the toroidal plasma current $I_p = -30MA$ and the volume average $\beta = 7.3\%$ remain fixed. Ideal global external kink modes are weakly unstable but indicate stability for $I_{hc} > 138MA$. The local ideal magnetohydrodynamic stability criteria are satisfied in the range $42MA < I_{hc} < 122MA$. The peaked toroidal current generates local maxima of the modulus of the magnetic field strength in the central region of the plasma which has very favourable implications for energetic and thermal particle confinement. This is confirmed through the computation of a very small α-particle guiding centre orbit loss fraction.

1 INTRODUCTION

Magnetic fusion offers the potential of a clean and everlasting source of energy to satisfy the requirements of humankind. For a plasma to ignite and burn, typically its density must be $n \sim 10^{20} particles/m^3$, its temperature must reach $T \sim 10keV$ and the confinement of the thermal particle energy must approach $\tau \sim 1s$. This is often combined to yield the criterion $nT\tau \sim 10^{21} kev - s/m^3$ for a relevant power plant. First generation reactors are anticipated to rely on Deuterium (D_1^2) and Tritium (T_1^3) as the reaction

$$D_1^2 + T_1^3 \longrightarrow n_0^1 + He_2^4 + 17.6MeV \tag{1}$$

constitutes the easiest to realise experimentally. The energy carried by the neutron that can be recovered in a blanket surrounding the discharge chamber amounts to $14.1Mev$ per reaction. The heat generated in the blanket as the neutron delivers its energy through collisions with the structure in turn can run a conventional turbine. The $3.5MeV$ α particles (the helium nuclei) remain confined in the plasma as they are electrically charged and provide the source of energy required to sustain the plasma temperature through collisional processes with the background plasma particles and the generation of waves that may also interact with the plasma fluid.

The cost of a magnetic fusion reactor is closely linked with the magnetic field required to confine the plasma. The magnitude of this field, labelled B, depends on the current that must be driven in the coils which in turn dictates the size of the coils, the material from which they must be constructed and the cooling capabilities. Magnetohydrodynamic (MHD) instabilities can be triggered whenever the B-field strength becomes too weak. Specifically, instabilities can arise when the ratio of the kinetic pressure of the confined gas to the magnetic pressure of the confining fields exceeds a critical value. This parameter is defined as β,

$$\beta = \frac{2\mu_0 \int d^3xp}{\int d^3xB^2} \ . \tag{2}$$

The kinetic pressure p is proportional to the product nT and the requirement for fusion reaction that this product approach $10^{20} keV/m^3$ entails that B must be sufficiently large to avoid instabilities that can destroy the plasma column.

It has been demonstrated theoretically and experimentally in a Tokamak plasma confinement system that the maximum stable β values that can be achieved increase with decreasing aspect ratio. The aspect ratio $A = R/a$ is the ratio of the major radius to the minor radius. The major radius R is the distance from the major axis to the centre of the plasma column and the minor radius a is the average radius of the plasma column. As $A \rightarrow 1$, β values in excess of 15% can be realised. However, in a reactor concept, the necessity to shield the coil structure and the central column to neutron bombardment makes any design with low aspect ratio extremely difficult to fulfill.

The Tokamak systems utilise the coils to produce the longitudinal magnetic field the long way round the torus and a plasma current to generate the poloidal field the short way around the torus. This combination of fields serves to confine the charged particles in the plasma. The resulting magnetic field structure maintains a very high degree of symmetry in the toroidal direction. Stellarator systems can generate the confining fields entirely with external coils but usually at the expense of the symmetry in the toroidal direction. An investigation of α-particle orbits in nonsymmetric Stellarators reveals that a large fraction of them are lost almost instantaneously due to enhanced magnetic gradient and curvature drift effects and thus cannot contribute to the sustainment of the background plasma temperature. New Stellarator designs have been identified which, although three-dimensional (3D) in physical appearance, can still produce a magnetic field structure that resembles that of a two-dimensional Tokamak. These are known as quasiaxisymmetric Stellarators [1]. Furthermore, other 3D systems have been conceived such as the Wendelstein VII-X in construction in Germany that guarantee adequate confinement of α-particles through the poloidal closure of the second adiabatic invariant. These are referred to as quasi-isodynamic systems [2].

To highlight the principal physics issues in magnetic fusion reactor systems, MHD instabilities impose a limit on β which implies that the magnetic field B must have a minimum value. Furthermore, the confinement of α particles imposes an adequate level of symmetry properties in the magnetic field structure in addition to constraints on the magnitude of B. On the other hand, cost constraints favour systems that can satisfy the physics criteria (β, α-particle confinement) at the lowest possible B. One of the challenges of fusion physicists is to identify configurations and scenarios that optimally meet these conflicting conditions.

2 THE SPHELLAMAK CONCEPT

The Sphellamak concept [3], developed at CRPP/EPFL in collaboration with T. N. Todd of Culham Laboratories, UK, is a hybrid system that combines features of a Tokamak, a Stellarator and a Spheromak. A Spheromak is a coreless device that carries a toroidal current and relies on plasma instabilities and turbulence to generate the necessary toroidal magnetic field for confinement through a process of helicity conservation called the 'dynamo' action. The Sphellamak, like the Spheromak, is a coreless concept that employs Stellarator windings on a spheroidal surface. These coils produce seed paramagnetism that is significantly amplified by the toroidal plasma current. As the system is 3D, charge conservation ($\boldsymbol{\nabla} \cdot \boldsymbol{j} = 0$, where $\mathbf{j}$ is the plasma current density) implies that the toroidal plasma current generates not only the poloidal magnetic field, but also the toroidal magnetic field without a need for the dynamo effect and the instabilities associated with it. One of the main attractions of the Sphellamak is the potential to realise a very low aspect ratio device in a reactor as the absence of a central column eliminates the need for internal shielding. A reactor-sized version of a Sphellamak device is displayed in Figure 1. The helical coils are shown in red. The current in them flows up one leg, across the connecting arc segment near the upper pole, down the adjacent helical leg and then back across the arc segment near the lower pole. There are 10 modular coils in this device. The vertical field coils in blue near the polar regions carry half the current of the helical coils, but in the direction opposite that of the flow in the neighbouring arc segments to cancel the effective vertical fields produced by the circulation of currents in these arcs. The vertical field coils in yellow control the plasma position and counteract the outward hoop force induced by the toroidal current in the plasma. The distribution of B^2 on the outermost flux surface in shades of yellow, green and red appears within the coil structure.

3 MAGNETOHYDRODYNAMIC EQUILIBRIA

The free boundary version of the 3D VMEC equilibrium code [4] is employed to numerically compute Sphellamak equilibrium sequences. This code imposes perfectly nested magnetic flux surfaces like the layers of an onion on a doughnut shaped system for the equilibria that are calculated. The input required for this code are the radial, vertical and toroidal components of the vacuum magnetic fields produced by the currents in the external coil windings, the pressure and current profiles. Also required are the magnitudes of the toroidal magnetic flux $2\pi\Phi(1)$, the pressure at the magnetic axis $p(0)$ and the total toroidal current enclosed within the last flux surface $2\pi J(1)$. The contribution of the helical coils to the vacuum fields are computed using the Biot-Savart law on a toroidal domain of rectangular cross section within the helical coils, where each coil is modelled as a short straight segment. Four filaments, separated by a distance of $0.75m$ are employed to model the finite dimensions of these coils. The elliptic integral formulation of the Biot-Savart law is applied to determine the contributions of the vertical field coils to the vacuum magnetic field which are composed of four circular filaments separated by a distance of $0.375m$. A sequence of configurations have been calculated by varying the current in the helical coils from $42MA$ to $122MA$. The outer vertical field coil currents are adjusted to carry a 1/15 fraction of the helical coil current.

The VMEC code also requires the pressure profile which we have prescribed as

$$p(s) = p(0)(1 - s^2)^2 \tag{3}$$

where we have varied $p(0)$ to maintain $\beta = 7.3\%$ and the toroidal current profile

$$2\pi J'(s) = 2\pi J'(0)(3(1 - s)^5 + (1 - s^5)^2)/4 \tag{4}$$

where $0 \leq s \leq 1$ is the radial variable that labels the flux surfaces and is proportional to the volume enclosed. The value of $2\pi J'(0)$ is chosen such the the total toroidal current within the plasma is $-30MA$. An initial guess is provided for the shape of the plasma and the toroidal magnetic flux at the boundary $2\pi\Phi(1)$ is varied until a converged equilibrium is obtained.

The plasma volume and the average magnetic energy density in the plasma are displayed in Figure 2 for the sequence of equilibria investigated as a function of the current in the helical coils I_{hc}. The plasma volume decreases and the average magnetic energy increases with increasing helical coil current.

4 MAGNETOHYDRODYNAMIC STABILITY

We apply the local and global modules of the 3D ideal MHD stability code TERPSICHORE [5] to investigate Mercier, ballooning, internal and external kink modes modes of the Sphellamak sequence of equilibrium configurations. The TERPSICHORE code performs a coordinate transformation of the VMEC equilibria to Boozer magnetic coordinates [6]. These coordinates facilitate the evaluation of stability properties because the magnetic field lines become straight which simplifies the inversion of the $\boldsymbol{B} \cdot \boldsymbol{\nabla}$ operator and because the parallel current density, which is an important source of free energy for instabilities, can be more efficiently calculated.

The local stability modules of TERPSICHORE determine the Mercier criterion and the Fourier coefficients of the driving and stabilising terms that determine ballooning stability. Mercier modes are instabilities that are very localised about a magnetic surface but have extended structures along the magnetic field lines. Ballooning modes form structures that are localised along magnetic field lines typically in the region where the directions of the magnetic field line curvature and the pressure gradient become aligned, which is usually radially away from the major axis. The ballooning coefficients are reconstructed along the magnetic field lines and a shooting method is applied to evaluate the eigenvalue of the second order ordinary differential equation that describes ballooning stability. The Mercier criterion and the ballooning eigenvalue profiles as a function of the radial variable s are presented for the two limiting configurations of the sequence in Figure 3. Ignoring the very edge of the plasma where a slight flattening of the pressure profile will stabilise the ballooning eigenvalues, we observe that the Mercier criterion predicts unstable conditions for the system with helical coil current $I_{hc} = 42MA$ in the central region of the plasma but is otherwise stable to ballooning modes. On the other hand, the configuration with $I_{hc} = 122MA$ is Mercier stable but becomes weakly unstable in the region around $s \simeq 0.75$ (at 3/4 of the plasma volume). The intermediate configurations of the sequence are all stable. The spikes observed in the Mercier criterion are not considered as indicative of instability but rather of conditions whereupon the pressure gradient drives the formation of magnetic islands. Though this technically violates the condition of magnetic surface nestedness, these spikes are sufficiently localised and nonoverlapping that the assumption that guides the application of the VMEC code remains valid under these circumstances.

The global stability modules of the TERPSICHORE code serve to calculate unstable eigenvalues associated with current driven instabilities and pressure driven ballooning/interchange modes. Global mode structures are anticipated to have more deleterious consequences than local modes because they can produce vortices that connect the central region of the plasma to the edge and as a result destroy the plasma column. In Figure 4, we show the unstable eigenvalue with respect to the family of unstable $n = -1$ global eigenstructures as a functon of I_{hc}. The sequence we investigate is unstable in the range $42MA < I_{hc} < 122MA$, but from extrapolation we can predict a nearby case that is marginally stable at $I_{hc} \simeq 138MA$. We also present in this Figure the 4 dominant Fourier amplitudes of the radial component of the displacement vector for the case obtained with $I_{hc} = 102MA$. The internal region of the plasma is dominated by the $m = 1, n = -1$ term, where m is the poloidal mode number and $n = -1$ is the toroidal mode number. However, near the edge of the plasma, the $m = 2, 3$ terms become important because the $m = 1$ term becomes nearly vanishing there. The perturbed magnetic field is related to the displacement vector through the equation $\boldsymbol{\delta B} = \boldsymbol{\nabla} \times (\boldsymbol{\xi} \times \boldsymbol{B})$ from which we obtain $\sqrt{g}\delta B^s = \sqrt{g}\boldsymbol{B} \cdot \boldsymbol{\nabla}\xi^s$, where $\sqrt{g}$ is the Jacobian, and δB^s and ξ^s are the radial components of the perturbed magnetic field and the displacement vector, respectively. The quantity $\sqrt{g}\delta B^s$ is displayed an a flux surface very near the edge of the plasma for the $I_{hc} = 102MA$ case which confirms that a combination of $m/n = 2/-1$ and $m/n = 3/-1$ components form the eigenstructure. It is relevant because magnetic probes external to the plasma can be used to detect structures of this type.

5 THE MAGNETIC FIELD STRUCTURE

In typical Tokamak axisymmetric systems, the magnetic B-field strength is inversely proportional to the distance from the major axis. In classical Stellarators, the B-field strength becomes 3D and the magnetic drifts of trapped energetic particles cause them to quickly escape the plasma. In the Sphellamak device, the strong toroidal plasma current plays a critical rôle in generating the magnetic fields. With peaked toroidal current profiles, the magnetic field structure can acquire properties of a maximum-B system which are characterised by the B-field strength developing a local maximum in the central region of the plasma. The sequence of configurations we have investigated do in fact satisfy these conditions. The distribution of the modulus of B^2 (mod-B^2) on three different cross sections of the plasma (corresponding to the toroidal angles $\phi = 0$, $\pi/20$ and $\pi/10$) are displayed in Figure 6 for the configurations obtained with $I_{hc} = 42MA$ and $I_{hc} = 122MA$. The mod-B^2

distribution in the vicinity of the magnetic axis becomes closely aligned with the magnetic flux surfaces. This corresponds to a nearly isodynamic system [7] which has very favourable implications for confinement because the particle drifts remain confined within the flux surface [8].

6 α-PARTICLE GUIDING CENTRE ORBITS

The motion of electrically charged particles in a magnetic field is characterised by rapid gyration about a B-field line and streaming along it, but also by a slower drift across the field lines due to the inhomogeneity in B. In magnetic confinement systems where the typical scale length of the gyro-orbit is much smaller than characteristic scale lengths of the device, the guiding centre approximation, which averages over the gyromotion, can be invoked. This is the case of the Sphellamak equilibria we are considering. Thus the α-particle guiding centres rather than the exact orbits are followed. This reduces the problem to a much more tractable undertaking. The guiding centre motion can be described through a Hamiltonian formalism in which the Boozer magnetic coordinates constitute a canonical frame subject to the condition that the magnetic field is static with nested surfaces (and that time dependent general perturbations can be represented as the curl of a scalar function times the equilibrium magnetic field) [9]. Furthermore, the guiding centre orbit equations expressed in these coordinates depend on quantities that are constant on each flux surface and on the magnitude of B. Therefore all of the geometric effects of shaping on the orbits manifest themselves only and exclusively through the structure of B. It thus becomes possible to conceive of confinement systems with strong 3D geometry but where B becomes independent of one or possibly both of the angular variables.

We follow the trajectories of 4500 α-particle guiding centres that are *born* on the flux surface $s \simeq 0.25$ (at 1/4 the plasma volume) with a random distribution of pitch angle (the ratio of the parallel to the total velocity), poloidal and toroidal angles using the VENUS code [10]. These trajectories are followed for up to $0.05s$ which corresponds to half of a slowing down time for a $3.5MeV$ α-particle. We monitor the guiding centre orbits that reach the last closed magnetic flux surface and consider these as lost. The fraction of α-orbits that are lost are shown in Figure 7 for the two limiting configurations of the sequence examined. We observe that the α-particle confinement is virtually perfect for $I_{hc} < 122MA$, while less then 2% of the orbits are lost for the $I_{hc} = 122MA$ case. For this case, the α loss is referred to as prompt and corresponds to particles that drift rapidly out of the device. To understand these results, we refer back to Figures 2 and 6 where we notice that the local maxima of B^2 increases with I_{hc} ($B^2 \sim 30T^2 \rightarrow 45T^2$), while the plasma volume decreases from $702m^3 \rightarrow 480m^3$. Though the distribution of B^2 appears similar for the two limiting configurations of the sequence, the $I_{hc} = 122MA$ case appears to be slightly more 3D than the $I_{hc} = 42MA$ case. The combination of smaller volume and higher 3D shaping may be just sufficient enough to overcome the larger magnitude of B to cause the slight deterioration of α confinement for the $I_{hc} = 122MA$ case. Nevertheless, this level of loss would not compromise the viability of $I_{hc} \geq 122MA$ configurations as power producing reactor devices.

7 COMPUTATIONAL ISSUES

Five programmes have been employed in the computations presented. The COIL.SPHELL package evaluates the vacuum magnetic fields from the currents in the external coil segments using the Biot-Savart law. The VMEC code numerically determines 3D equilibria. It is based on an accelerated preconditioned spectral energy minimisation scheme. The stability code TERPSICHORE evaluates local and global MHD stability properties. For the global modes, it solves a special block pentadiagonal matrix eigenvalue equation using an inverse vector iteration technique to determine the eigenvalue and the eigenvector. The VVBAL code uses a shooting method to solve the ballooning mode eigenvalue. The VENUS code solves the guiding centre orbit equations using an initial value method that combines a 4th order Runge-Kutta solver with a 2nd order version. The time step is typically $10^{-8}s$.

The VMEC and TERPSICHORE codes have long vector lengths for which the use of vector/parallel supercomputers is most appropriate. Typical VMEC runs require less than $100Mbytes$ and take $\sim 1000s$ CPU time while TERPSICHORE runs require 0.5 to $1.5Gbytes$ and take $\sim 100 - 200s$ CPU time on a NEC/SX4 platform. The VENUS code is most effectively run on a massively parallel system as each guiding centre particle can be assigned to a different processor. A typical run consists of 4500 particles on 16 processors which takes about $1.5hours$ on an ORIGIN 2000 machine.

All graphics (1D $\rightarrow$ 3D) are undertaken in a post-process procedure on a PC utilising mostly MATLAB but sometimes BASPL routines. The Sphellamak coil system is designed with a MATLAB programme.

8 SUMMARY, CONCLUSIONS AND DISCUSSION

The ideal MHD stability and the α particle confinement properties of a Sphellamak reactor concept have been investigated. We have concentrated on a sequence of configurations where we have varied the current I_{hc} in the helical coils keeping a peaked toroidal plasma current at $-30MA$ and a volume average $\beta = 7.3\%$ fixed. The magnetic field strength B increases and the plasma volume decreases with raising I_{hc}. The local stability criteria improve with increasing I_{hc} in the inner half of the plasma volume and deteriorate in the outer half. The global ideal MHD kink mode imposed by the $n = -1$ family of instabilities becomes less unstable as I_{hc} is raised predicting a marginal point for the case $I_{hc} \sim 138MA$. The magnetic field structure displays local maxima of B in the central region throughout the range of configurations explored. These maximum-B equilibria have closed B-contours that become aligned with the magnetic flux surfaces. This has a very favourable impact on the confinement of α-particles as the magnetic drifts out of the flux surfaces are weak as confirmed by the computation of a very small α-guiding centre orbit loss fraction of less than 2%.

Although the set of Sphellamak configurations we have presented appears to constitute a very attractive example for a reactor system, further improvements in the ideal MHD stability properties are still required to guarantee a robust margin of stable operation as this sequence we have identified is not sufficiently satisfactory.

The very satisfactory α-particle confinement in the Sphellamak reactor configurations can be attributed to the maximum-B properties of the magnetic field structure around the centre of the plasma. This structure is realised with a peaked toroidal plasma current. One of the principal technical challenges beyond the scope of this article is how to generate and sustain such type of current profile and magnitude of current in the absence of a central column.

The satisfactory resolution of MHD stability and α-particle confinement is paramount in the evaluation of a viable reactor concept. However, as confined plasmas are not in general quiescent, other physics issues must eventually also be considered. Specifically, we have not addressed the issue of confinement of thermal particles in the background of a turbulent plasma that determines the plasma energy confinement that must approach $\tau \sim 1s$ in a reactor. These turbulent fields may also unfavourably impact the α-particle confinement.

Acknowledgments

This research was partially sponsored by the Fonds National Suisse de la Recherche Scientifique. We thank Dr. S.P. Hirshman for use of the VMEC equilibrium code. The numerical calculations on equilibrium and stability presented in this paper were performed on the NEC-SX4 computer at the Centro Svizzero di Calcolo Scientifico, Manno, Switzerland. The guiding centre orbit calculations were undertaken on the ORIGIN-2000 massively parallel computer at SIC-EPFL.

References

[1]J. Nührenberg, W. Lotz and S. Gori, *Quasi-axisymmetric Tokamaks*, in Proc. Joint Varenna-Lausanne Int. Workshop on Theory of Fusion Plasmas, Editrice Compositori, Bologna (1994) 3-12.

[2] S. Gori and J. Nührenberg, *Quasi-isodynamic stellarators with magnetic well and positive shear*, in Proc. Joint Varenna-Lausanne Int. Workshop on Theory of Fusion Plasmas, Editrice Compositori, Bologna (1998) 473-480.

[3] W. A. Cooper, J. M. Antonietti and T. N. Todd, *A Paramagnetic Nearly Isodynamic Compact Magnetic Confinement System* in Proc. 17th IAEA Fusion Energy Conf., Yokohama, Japan, IAEA-CN-69/EX4/1(R) (1998).

[4] S. P. Hirshman, W. I. Van Rij and P. Merkel, *Three-dimensional free boundary calculations using a spectral Green's function method*, Computer Physics Communication **43** (1986) 143-155.

[5] D. V. Anderson, W. A. Cooper, R. Gruber, S. Merazzi and U. Schwenn, *Methods for the efficient calculation of the (MHD) magnetohydrodynamic stability properties of magnetically confined fusion plasmas*, The International Journal of Supercomputer Applications **4** (1990) 34-47.

[6] A. H. Boozer, *Establishment of magnetic coordinates for a given magnetic field*, Physics of Fluids **25** (1982) 520-521.

[7] D. Palumbo, Il Nuovo Cimento X **53B** (1968) 507.

[8] L. S. Hall and B. McNamara, *Three-dimensinal equilibrium of the anisotropic, finite-pressure guiding-center plasma: Theory of the magnetic plasma*, Physics of Fluids **18** (1975) 552-565.

[9] R. B. White and M. S. Chance, *Hamiltonian guiding center drift orbit calculation for plasmas of arbitrary cross section*, Physics of Fluids **27** (1984) 2455-2467.

[10] O. Fischer, W. A. Cooper and L. Villard, *Magnetic topology and guiding centre drift orbits in a reversed shear tokamak*, Nuclear Fusion **40** (2000) 1453-1462.

Figures

FIG. 1. The coil system of a Sphellamak reactor concept. The helical coils in red are wound on a spheroidal surface of $7.5m$ radius. The coil width is roughly $0.75m$. The vertical field compensation coils that cancel the current flowing in the arc segments that connect the helical coil legs are shown in blue. They carry half the current in the helical coils but in the opposite direction of that in the arc segments. The vertical field coils in yellow control the plasma position. The B^2 distribution on the outermost flux surface appears in shades of green, yellow and red. The Boozer magnetic coordinate grid is also shown.

FIG. 2. The plasma volume in m^3 (top) and the average magnetic energy density in *Pascals* (bottom) as a function of the helical coil current I_{hc} in MA of the sequence of equilibria expored with toroidal plasma current $I_p = -30MA$ and $\beta = 7.3\%$.

FIG. 3. The ballooning eigenvalue (top) and Mercier criterion (bottom) profiles for the two limiting configurations of the sequence of equilibria explored having $I_{hc} = 42MA$ and $I_{hc} = 122MA$, respectively.

FIG. 4. The global eigenvalue λ corresponding to the $n = -1$ family of instabilities as a function of the helical coil current I_{hc} of the sequence of Sphellamak equilibria investigated (top). The marginal point that is extrapolated has $I_{hc} \simeq 138MA$. The 4 leading Fourier components of the mode structure corresponding to the $n = -1$ instability family as a function of the radial variable s for the $I_{hc} = 102MA$ case of the sequence explored (bottom).

FIG. 5. The distribution of $\sqrt{g}\delta B^s$ on a flux surface very near the edge of the plasma for the $I_{hc} = 102MA$ case of the sequence of Sphellamak reactor equilibria explored.

FIG. 6. The B^2 distribution on cross sections at the beginning of a field period $\phi = 0$ (top), at one quarter of a field period $\phi = \pi/20$ (middle) and at half period $\phi = \pi/10$ (bottom) for the two limiting configurations of the sequence of Sphellamak equilibria explored with $I_{hc} = 42MA$ (left) and $I_{hc} = 122MA$ (right), respectively, in the Boozer magnetic coordinate frame.

FIG. 7. The fraction (in percent) of α-particle orbits lost in $0.05s$ (half of a $3.5MeV$) for the two limiting configurations of the Sphellamak reactor sequence explored with $I_{hc} = 42MA$ (in blue) and with $I_{hc} = 122MA$ (in red), respectively.

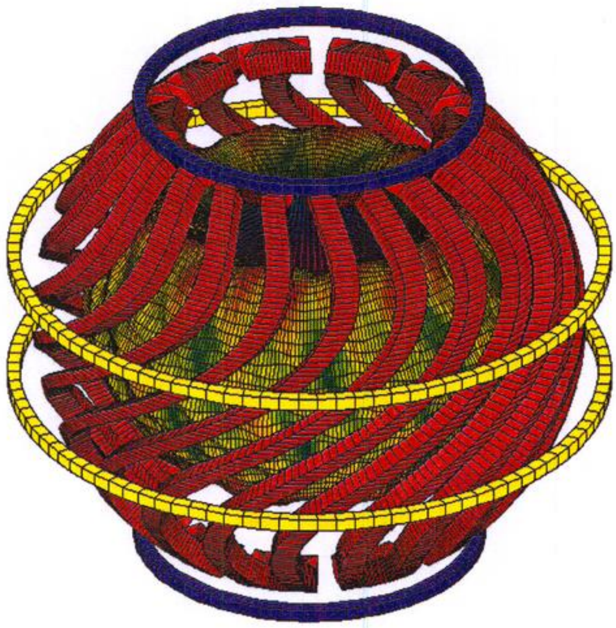

Fig. 1

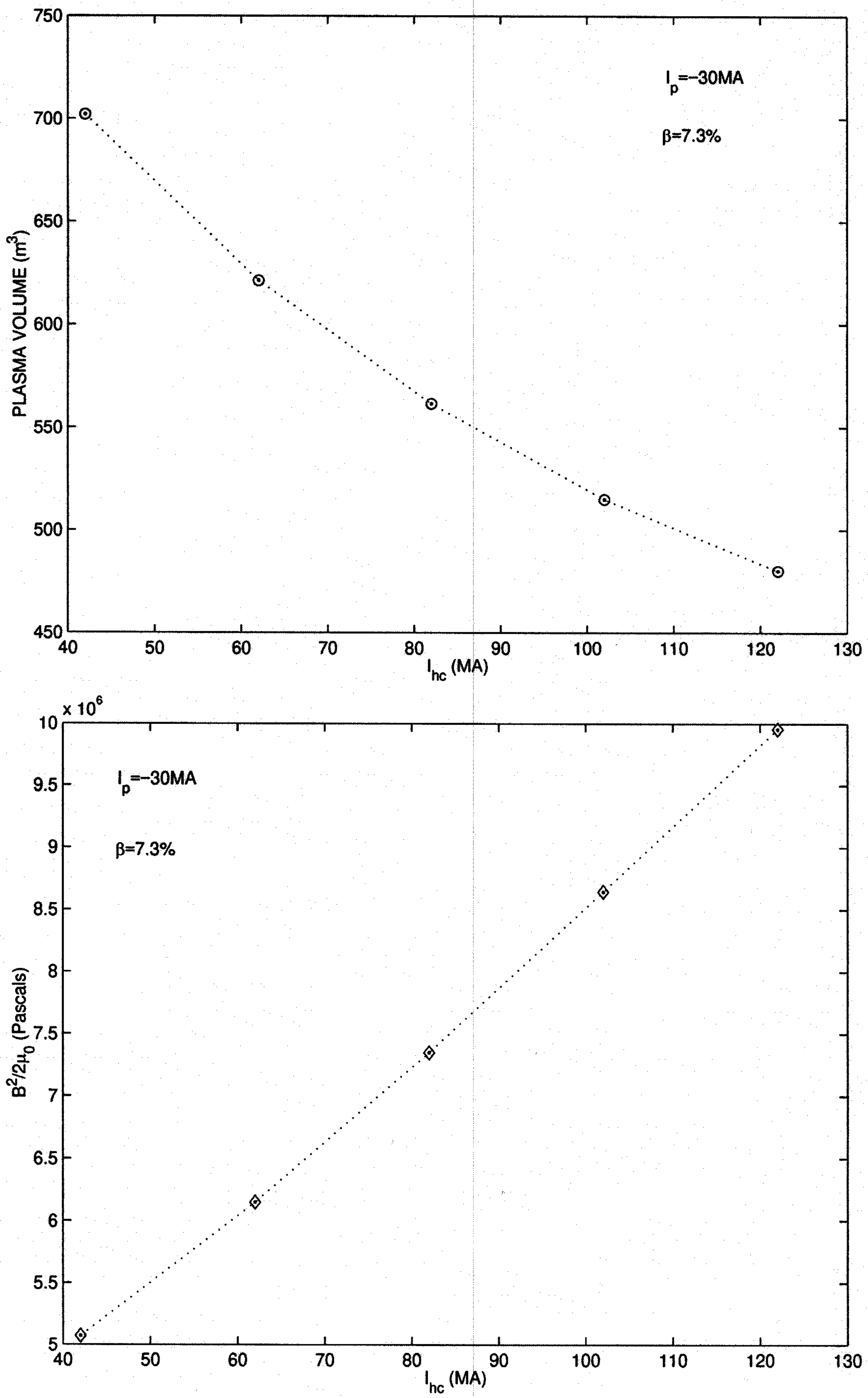
I_p=-30MA
β=7.3%
PLASMA VOLUME (m³)
I_hc (MA)
x 10⁶
I_p=-30MA
β=7.3%
B²/2μ₀ (Pascals)
I_hc (MA)

Fig. 2

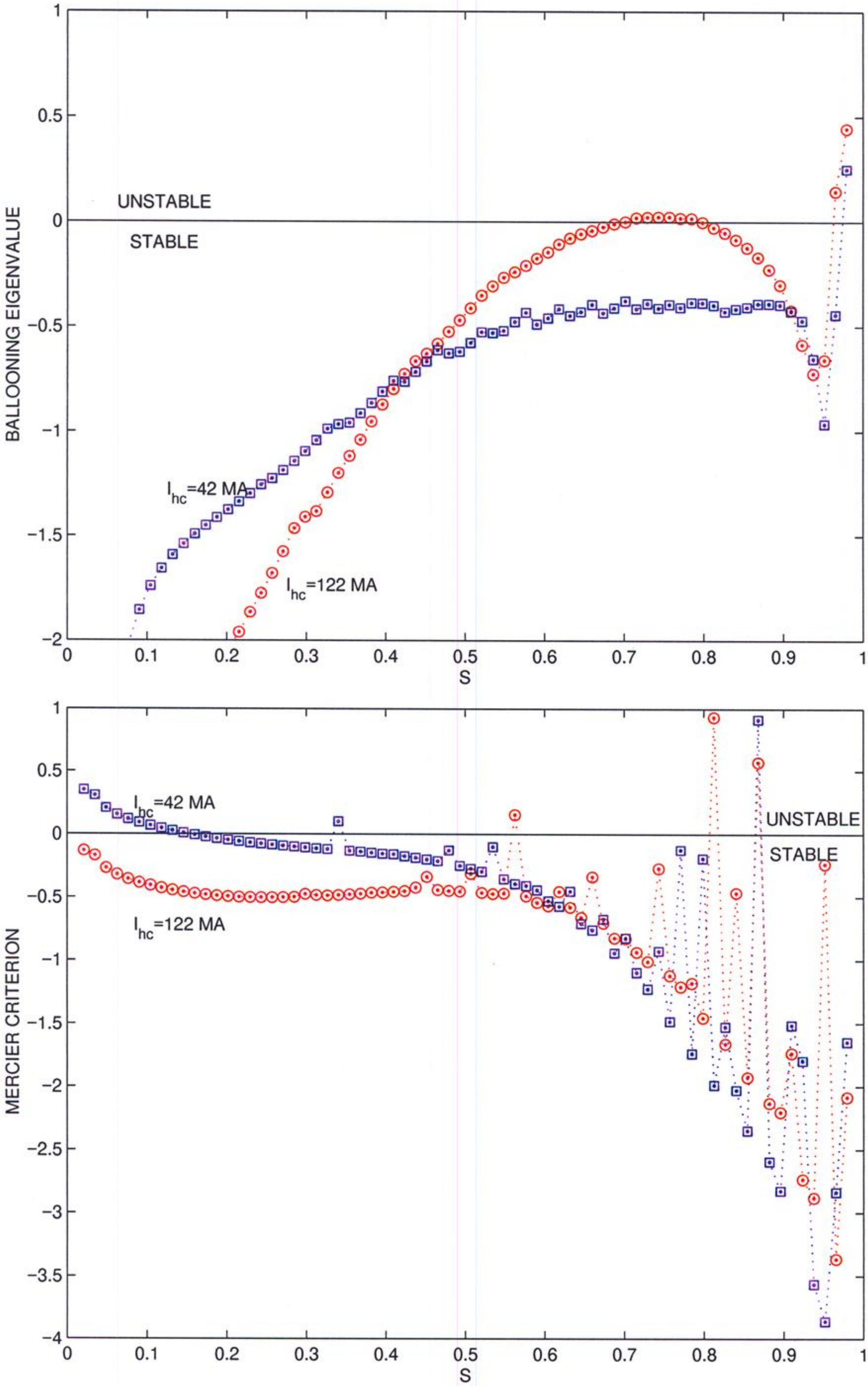

BALLOONING EIGENVALUE
UNSTABLE
STABLE
I_hc=42 MA
I_hc=122 MA
S
MERCIER CRITERION
I_hc=42 MA
UNSTABLE
STABLE
I_hc=122 MA
S

Fig. 3

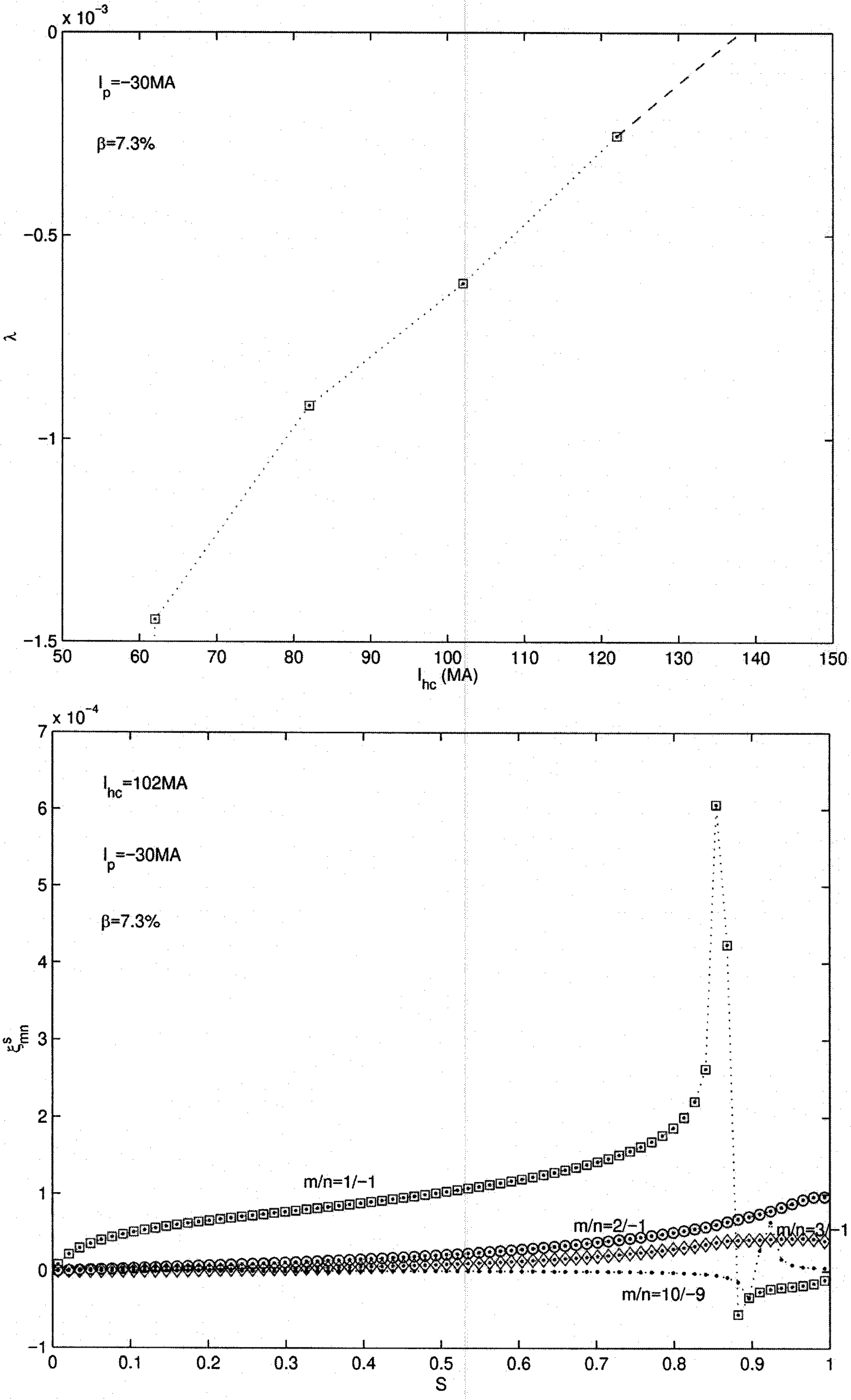
x 10^-3
I_p=-30MA
β=7.3%
λ
I_hc (MA)
x 10^-4
I_hc=102MA
I_p=-30MA
β=7.3%
ξ^s_mn
m/n=1/-1
m/n=2/-1
m/n=3/-1
m/n=10/-9
S

Fig. 4

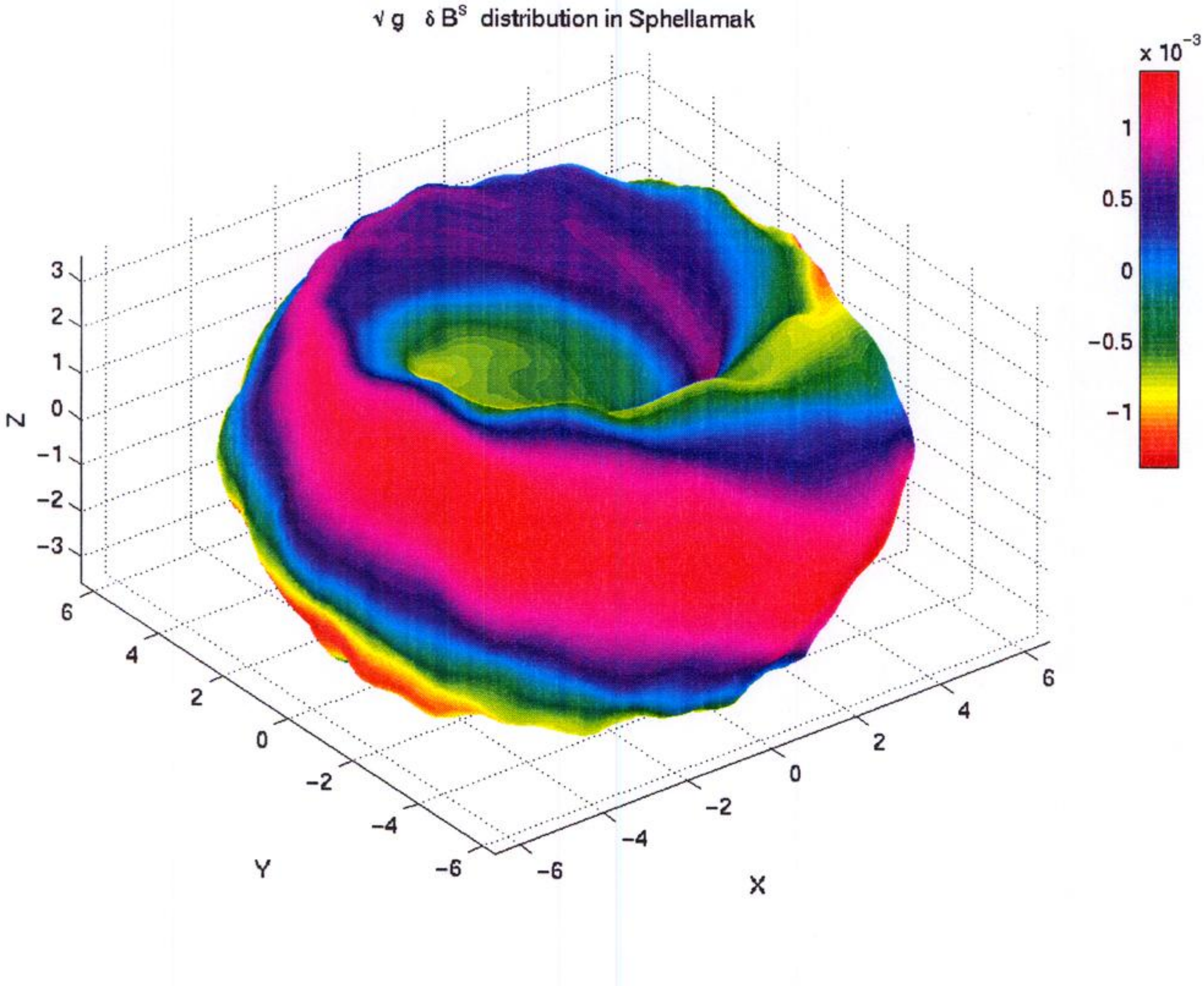
√g δB^s distribution in Sphellamak
x 10^-3
1
0.5
0
−0.5
−1
Z
3
2
1
0
−1
−2
−3
Y
6
4
2
0
−2
−4
−6
X
−6
−4
−2
0
2
4
6

Fig. 5

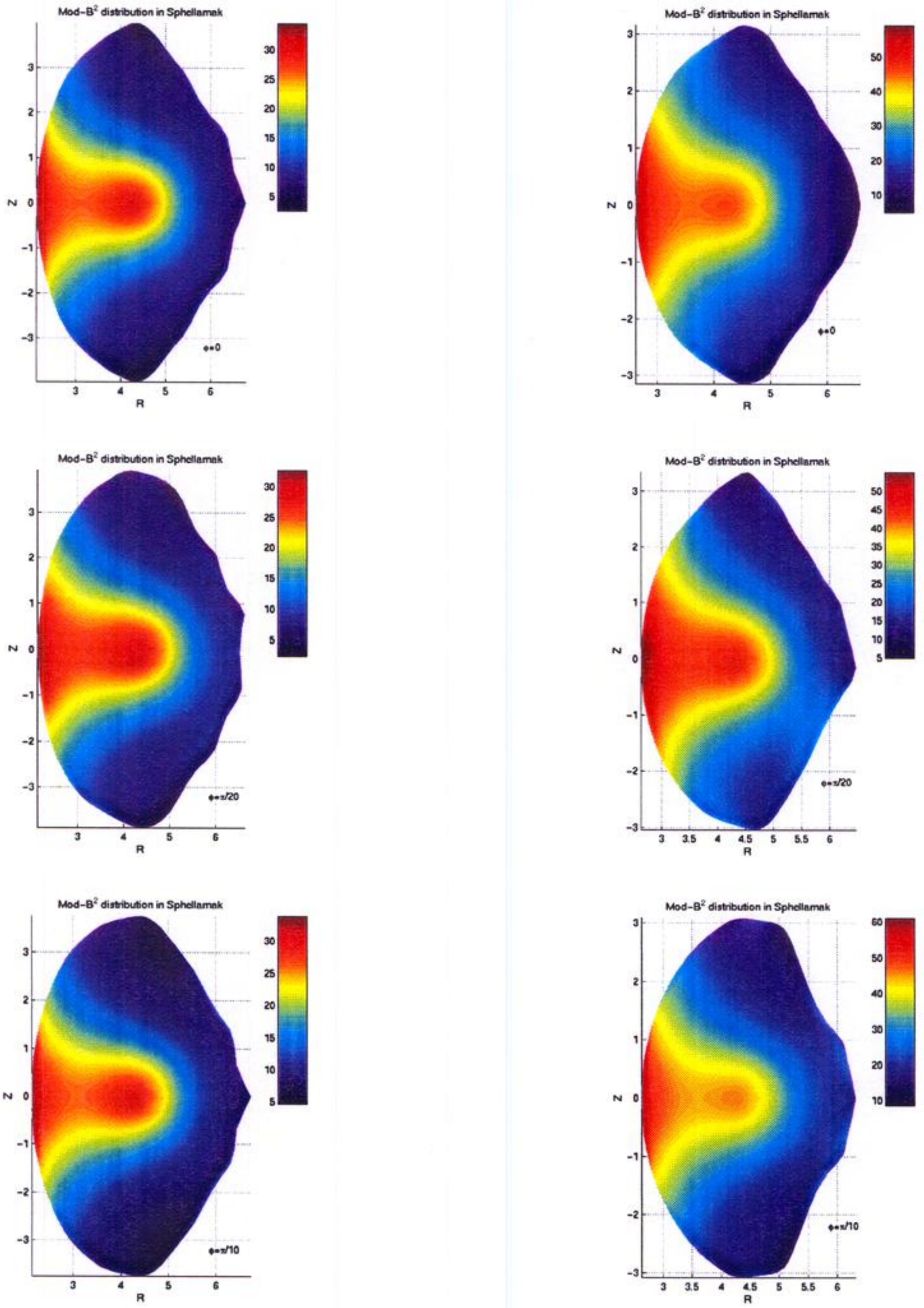

Fig. 6

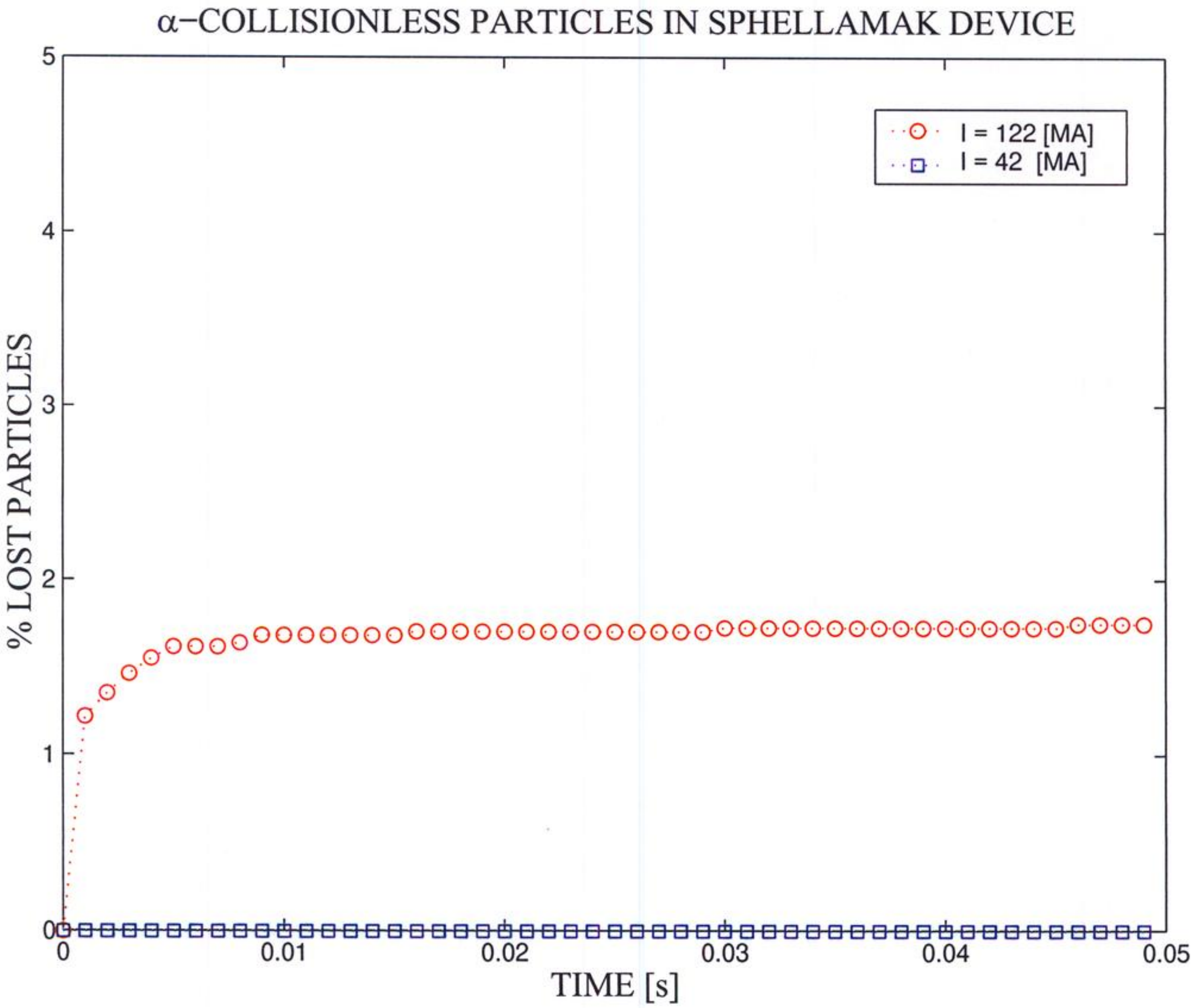
α−COLLISIONLESS PARTICLES IN SPHELLAMAK DEVICE
I = 122 [MA]
I = 42 [MA]
% LOST PARTICLES
TIME [s]
0
1
2
3
4
5
0.01
0.02
0.03
0.04
0.05

Fig. 7